ELSEVIER

Journal of Organometallic Chemistry 657 (2002) 40–47

Journal of Organometallic Chemistry

www.elsevier.com/locate/jorganchem

Chemistry on a metallathiaborane cluster Part 4☆: reactions of 11-vertex rhodathiaboranes with bidentate phosphines and their subsequent rearrangements

Oleg Volkov [1], Ramon Macias, Nigam P. Rath, Lawrence Barton *

Department of Chemistry, Center for Molecular Electronics, University of Missouri-St. Louis, St. Louis, MO 63121, USA

Received 3 September 2001; accepted 15 February 2002

Abstract

The phosphine ligands on [8,8-$(PPh_3)_2$-*nido*-8,7-$RhSB_9H_{10}$] (**I**) may be replaced by the bidentate phosphines, $(CH_2)_n(PPh_2)_2$, to form species of the type [8,8-{η^2-$(CH_2)_n(PPh_2)_2$}-8-{η^1-$(CH_2)_n(PPh_2)_2$}-*nido*-8,7-$RhSB_9H_{10}$] (**II**), in the case of dppm ($n = 1$) and of the type [8,8-{η^2-$(CH_2)_n(PPh_2)_2$}-*nido*-8,7-$RhSB_9H_{10}$] (**III**), in the case of dppe ($n = 2$) and dppp ($n = 3$). It was originally thought that the chemistry followed by dppm differed substantially but predictably from that of dppe and dppp. In fact the reactions are more complex and mixed-ligand systems are accessible which provide insight into these reactions and rearrangement mechanisms. Reactions involving the transfer of a metal bonded bidentate phosphine to the cage are observed for dppe and dppp but only for dppm can a species of the type [1-PPh_3-{1,3-(μ-dppm)}-*closo*-1,2-$RhSB_9H_8$] (**IV**), which may be the key to the identification of the intermediate in these reactions, be observed. We also observed the ultimate product in this series of reactions which appears to be a mixture of isomers, [3-(η^1-dppm)-1,1-(η^2-dppm)-*closo*-1,2-$RhSB_9H_8$] (**V**) and [1-(η^1-dppm)-1,3-(μ-dppm)-*closo*-1,2-$RhSB_9H_8$] (**VI**). Additional ligand exchange reactions can be effected so that such species as [3-(η^1-dppm)-1,1-(η^2-dppe)-*closo*-1,2-$RhSB_9H_8$] (**VII**) may be isolated from **IV**. From these results, suggestions for possible reaction pathways are presented. © 2002 Published by Elsevier Science B.V.

Keywords: Boranes; Metallaboranes; Thiaboranes; Rhodium; NMR spectroscopy; X-ray diffraction

1. Introduction

The related pair of metallaheteroboranes, [9,9-$(PPh_3)_2$-*nido*-9,7,8-$RhC_2B_8H_{11}$] (**VIII**) [2] and [8,8-$(PPh_3)_2$-*nido*-8,7-$RhSB_9H_{10}$] (**I**) [3], compounds which are formally isoelectronic, are two electrons short of the number notionally required to satisfy the polyhedral skeletal electron pair theory [4]. The latter rhodathiaborane, **I**, is stable, easily prepared, and had been the more extensively studied of the two prior to our previous work on this system [3,5–8]. There are novel features associated with compound **I**. Structural and calculational studies have suggested the presence of two unusual *ortho*-CH...Rh agostic interactions [5] which, it is suggested, account for its stability. **I** undergoes interesting fluxional behavior in solution and is reactive towards both electrophiles and nucleophiles [3]. In particular, the reactions of **I** with Lewis bases, L, (where L = CO, PMe_2Ph or CH_3CN) result in either addition of the ligand, L, to the metal center or addition and substitution, giving rise to species such as [8-L-8,8-$(PPh_3)_2$-*nido*-8,7-$RhSB_9H_{10}$] (where L = CO [3b] or CH_3CN [4]) and [8,8,8-$(PMe_2Ph)_3$-*nido*-8,7-$RhSB_9H_{10}$] [6]. Refluxing [8-(CO)-8,8-$(PPh_3)_2$-*nido*-8,7-$RhSB_9H_{10}$] in benzene leads to the formation of [1-(CO)-1,3-$(PPh_3)_2$-*closo*-1,2-$RhSB_9H_8$], which when treated with an excess of PMe_2Ph, also in refluxing benzene, affords [1-(CO)-1-(PMe_2Ph)-3-L-*closo*-1,2-$RhSB_9H_8$] (where L = PMe_2Ph or PPh_3) [3b]. Other reaction patterns

---

☆ See Ref. [1].

* Corresponding author. Fax: +1-314-516-5342.

E-mail address: lbarton@umsl.edu (L. Barton).

[1] Permanent address: Institute of Inorganic Chemistry, Russian Academy of Sciences, 630090, Novosibirsk, Russia.

0022-328X/02/$ - see front matter © 2002 Published by Elsevier Science B.V.
PII: S0022-328X(02)01329-3

such as terminal hydrogen substitution at the 9-position by an OEt group [7] or metal incorporation to form 12-vertex bimetallic species have also been reported [3b]. Our previous work on this system described a study of the reactions of **I** with the bidentate *bis*(diphenylphosphino)alkanes, $[(CH_2)_n(PPh_2)_2]$, where $n = 1$, 2 and 3, (abbreviated as dppm, dppe and dppp, respectively) [1b]. Some of the results are illustrated in Scheme 1. It appeared that the reactions with dppm differed from those with dppe and dppp. For the former, the species [8,8-(η^2-dppm)-8-(η^1-dppm)-*nido*-8,7-$RhSB_9H_{10}$] (**II**), which contained both mono- and bidentate-dppm ligands on Rh, was isolated, and although other species clearly existed in the reaction mixture, we were unable to isolate them. Derivative chemistry at the pendant PPh_2 group in **II** was demonstrated by the formation of [8,8-η^2-{η^2-(BH_3)dppm}-*nido*-8,7-$RhSB_9H_{10}$] (**IX**) on reaction with $BH_3\cdot THF$ [1a] and [8,8-η^2-{(μ-Cl)$_2$Ru(η^6-*p*-cym)$Ph_2PCH_2PPh_2$}-*nido*-8,7-$RhSB_9H_{10}$] on reaction with [Ru(η^6-*p*-cym)Cl_2]$_2$ [1c]. With dppe or dppp, the analogue of **II** is not observed but species of the type [8,8-(η^2-dppp)-*nido*-8,7-$RhSB_9H_{10}$] (**III**) containing a single bidentate ligand on Rh, and one containing two ligands, [8,8-(η^2-dppp)-9-(η^1-dppp)-*nido*-8,7-$RhSB_9H_{10}$] (**X**) one of them on the cage, as illustrated in Scheme 1, are precursors to *closo*-clusters of the type [1,1-(η^2-dppp)-3-(η^1-dppp)-*closo*-1,2-$RhSB_9H_8$] (**XI**) and more complex linked clusters [1b]. In this paper, we report additional progress in this area.

2. Experimental

2.1. General

Solvents used were reagent grade and were dried before use. Some reactions were carried out using a Schlenk line, a glove box and standard techniques for handling air-sensitive compounds [9]. [8,8-$(PPh_3)_2$-*nido*-8,7-$RhSB_9H_{10}$] (**I**) was prepared according to the literature method [3b] from the reaction between Cs[SB_9H_{12}] [10] and [RhCl$(PPh_3)_3$] [11]. PPh_3 and dppe were obtained from Aldrich and dppm was obtained from Strem. NMR spectroscopy was carried out on a Bruker ARX 500 spectrometer operating at 500.1 MHz for proton, 160.5 MHz for boron-11, and at 202.5 MHz for phosphorus-31. Chemical shifts are reported in ppm for CD_2Cl_2 solutions to low field (high frequency) of $Et_2O\cdot BF_3$ for ^{11}B, of $SiMe_4$ for ^{1}H and of 85% H_3PO_4 for ^{31}P. Elemental analyses were attempted by Atlantic Microlabs Inc., Norcross, GA. NMR spectra were run on all samples sent for mass spectra and crystal growth was generated from NMR samples, after spectral analysis. The samples were evaporated to dryness and then dissolved in the appropriate solvent for subsequent crystallization. The mass spectra were measured in the FAB mode on a JEOL MStation JMS-700 spectrometer using 3-nitrobenzyl alcohol (3-NBA).

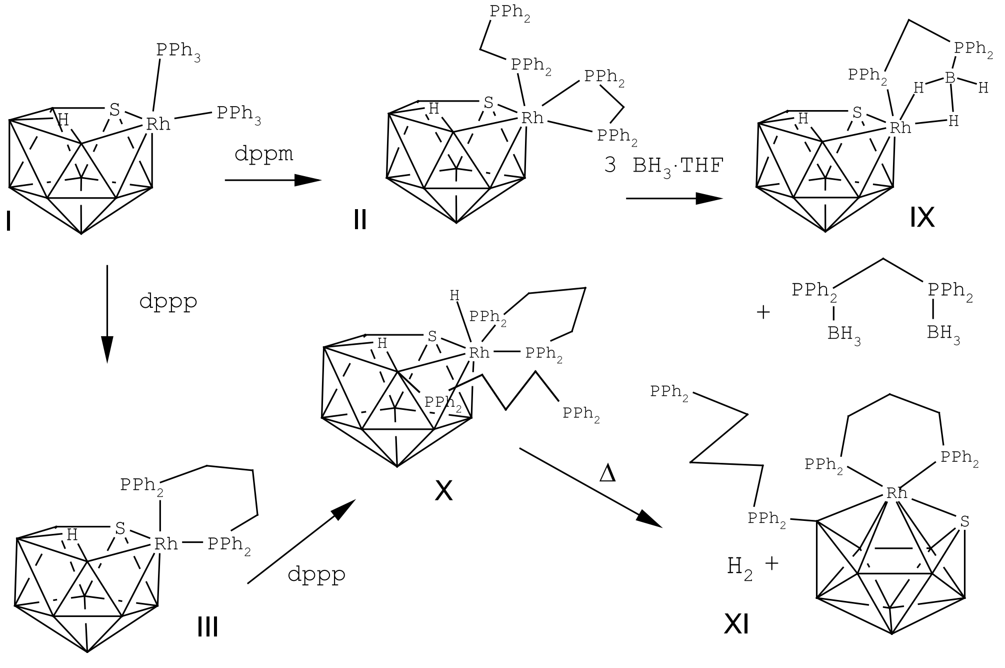

Scheme 1.

2.2. Preparation of [1-(PPh_3)-{1,3-(μ-dppm)}-closo-1,2-$RhSB_9H_8$] (IV)

[8,8-$(PPh_3)_2$-*nido*-8,7-$RhSB_9H_{10}$] (**I**) (53 mg, 0.069 mmol) was added to a solution of [8,8-(η^2-dppm)-8-(η^1-dppm)-*nido*-8,7-$RhSB_9H_{10}$] (**II**) (70 mg, 0.069 mmol) in CH_2Cl_2 (*ca.* 10 ml) under N_2. The reaction mixture was stirred at room temperature (r.t.) for 3 days. After this time, the solvent was reduced in volume and the reaction mixture was applied to the Chromatotron (a radial chromatograph obtained from Harrison Research, Palo Alto, CA) using a 25 cm diameter circular plate coated with 0.1 cm of silica gel (EM Science) using CH_2Cl_2–hexane (3:2) mixture as the mobile phase. A red compound was isolated and characterized as [1-(PPh_3)-{1,3-(μ-dppm)}-*closo*-1,2-$RhSB_9H_8$] (**IV**) (0.075 g, 0.084 mmol; 61%). Single crystals of this material were obtained by slow diffusion of EtOH into CH_2Cl_2 solution. Anal. Calc. for $C_{43}H_{45}B_9P_3RhS$: C, 58.23; H, 5.11. Found: C, 58.33; H, 5.17%. HR-MS (FAB with 3-NBA) *m*/*z* Calc. for $C_{43}H_{45}B_9P_3RhS$: 887.2412 $[M]^+$; Found: 887.2432. The observed and calculated mass envelopes for the measured masses are, {*m*/*q*, observed intensity (Calc. intensity)}: 884, 15.5 (15.22); 885, 56.7 (43.39); 886, 75.2 (82.57); 887, 100.00 (100.00); 888, 68.5 (70.72); 889, 35.6 (26.82); 890, 13.3 (7.58). ^{11}B-NMR (160.5 MHz, CD_2Cl_2, 25 °C): δ 34.9 (d, J(P,B) = 134 Hz, 1B), 20.8 (d, J(H,B) = 179 Hz, 1B), 5.4 (v br, 1B), −9.2 (v br, 2B), −20.0 (v br, 2B), −29.4 (v br, 2B). ^{31}P{^{1}H}-NMR (202.5 MHz, CD_2Cl_2, 25 °C): δ 47.2 (dd, J(P,Rh) = 135 Hz, J(P,P) = 31 Hz, 1P), 45.8 (ddd, J(P,Rh) = 172 Hz, J(P,P) = 96 Hz, J(P,P) = 31 Hz, 1P), 17.1 (m, 1P). ^{1}H-NMR (500 MHz, CD_2Cl_2, 25 °C): δ 7.70–6.97 (m, 35H; C_6H_5), 3.71 (t, J(P,H) = 10 Hz, 2H; $Ph_2P\mathit{CH_2}PPh_2$). Additional ^{1}H{^{11}B}-NMR (500 MHz, CD_2Cl_2, 25 °C): δ 3.60 (br, 2H, BH), 2.32 (2H, BH), 0.42 (v br, 4H, BH).

2.3. Preparation of [3-(η^1-dppm)-1,1-(η^2-dppe)-closo-1,2-$RhSB_9H_8$] (VII)

To a solution of [1-(PPh_3)-{1,3-(μ-dppm)}-*closo*-1,2-$RhSB_9H_8$] (**IV**) (0.020 g, 0.023 mmol) in 5 ml CH_2Cl_2 was added dppe (0.013 g, 0.033 mmol) under N_2. This reaction mixture was stirred at r.t. for 1 h. A yellow compound precipitated when EtOH was added, which was characterized as [3-(η^1-dppm)-1,1-(η^2-dppe)-*closo*-1,2-$RhSB_9H_8$] (**VII**) (0.021 g, 0.02 mmol; 87%). Crystals suitable for X-ray analysis were grown by layering a CH_2Cl_2 solution of the product with pentane. Anal. Calc. for $C_{51}H_{54}B_9P_4RhS$: C, 59.87; H, 5.32. Found: C, 59.23; H, 5.36%. HR-MS (FAB with 3-NBA) *m*/*z* Calc. for $C_{51}H_{53}B_9P_4RhS$: 1022.2780 $[M\text{–}H]^+$; Found: 1022.2834. The observed and calculated mass envelopes for the measured masses are {*m*/*q*, observed intensity (Calc. intensity)}: 1019, 21.43 (14.46); 1020, 46.52 (41.61); 1021, 80.47 (80.43); 1022, 100 (100); 1023, 81.95 (74.37); 1024, 45.93 (31.18); 1025, 21.94 (9.53). ^{11}B-NMR (160.5 MHz, CD_2Cl_2, 25 °C): δ 36.3 (d, J(P,B) = 122 Hz, 1B), 27.1 (d, J(H,B) = 79 Hz, 1B), 1.2 (v br, 3B), −16.3 (v br, 2B), −27.4 (v br, 2B). ^{31}P{^{1}H}-NMR (202.5 MHz, CD_2Cl_2, 25 °C): δ 60.8 (d, J(P,Rh) = 144 Hz, 2P), 4.3 (v br, 1P), −25.8 (d, J(P,P) = 35 Hz, 1P). ^{1}H-NMR (500 MHz, CD_2Cl_2, 25 °C): δ 7.42–6.97 (m, 40H; C_6H_5), 2.99 (d, J(P,H) = 10 Hz, 2H; $Ph_2P\mathit{CH_2}PPh_2$), 2.52–2.41 (m, 2H; $Ph_2P\mathit{C_2H_4}PPh_2$), 2.24–2.16 (m, 2H; $Ph_2P\mathit{C_2H_4}PPh_2$). Additional ^{1}H{^{11}B}-NMR (500 MHz, CD_2Cl_2, 25 °C): δ 3.93 (1H, BH), 2.74 (1H, BH), 1.99 (2H, BH), 0.59 (2H, BH), −0.03 (2H,BH).

2.4. Preparation of the mixture of isomers [$(dppm)_2$-closo-1,2-$RhSB_9H_8$] (V) and (VI)

a) A solution of [8,8-(η^2-dppm)-8-(η^1-dppm)-*nido*-8,7-$RhSB_9H_{10}$] (40 mg, 0.040 mmol) in CH_2Cl_2 (ca. 10 ml) was stirred under N_2 for 7 days at r.t. After this time a red compound was precipitated by addition of pentane. Recrystallization in CH_2Cl_2–hexane gave rise to the isolation of a product, characterized as a mixture of isomers of [$(dppm)_2$-*closo*-1,2-$RhSB_9H_8$] (0.026 g, 0.026 mmol; 65%).

b) dppm (0.052 g, 0.135 mmol) was added to a solution of [1-(PPh_3)-{1,3-(μ-dppm)}-*closo*-1,2-$RhSB_9H_8$] (0.078 g, 0.088 mmol) in 15 ml CH_2Cl_2 under N_2 and the reaction mixture was stirred at r.t. After 2 h addition of 15 ml EtOH resulted in a precipitation of a red product, which was recrystallized from CH_2Cl_2–hexane and characterized after drying in vacuo as a mixture of isomers of [$(dppm)_2$-*closo*-1,2-$RhSB_9H_8$] (0.068 g, 0.067 mmol; 76%). HR-MS (FAB with 3-NBA) *m*/*z* calc. for $C_{50}H_{52}B_9P_4RhS$: 1009.2702 $[M]^+$; Found: 1009.2709. The mass envelopes for the measured masses match quite well with those calculated from the known isotopic abundances of the constituent elements and are as follows: {*m*/*q*, observed intensity (Calc. intensity)}: 991, 62.6 (32.4); 992, 87.7 (72.24); 993 (100.00) 100.00; 994, 92.6 (78.76); 995, 76.2 (31.3); 996, 48.1 (7.58). Anal. Calc. for $C_{50}H_{52}B_9P_4RhS$: C, 59.51; H, 5.19. Found: C, 59.52; H, 5.26%. NMR spectra of the mixture of isomers: ^{11}B-NMR (160.5 MHz, CD_2Cl_2, 25 °C): δ 26.9 (br, m, P*B*, 2B), 14.13 (br, 2B), 9.51 (br, 2B) 6.91 (br, 2B), 2.49 (br, 3B), −1.78 (br, 1B), −7.24 (br, 1B), −13.07 (d, J(H,B) = 130 Hz, 2B), −21.10 (d, J(H,B) = 134 Hz, 3B). ^{1}H{^{31}P}-NMR (500 MHz, CD_2Cl_2, 25 °C): δ 8.16–6.23 (m, C_6H_5), 3.95 (br d, J(H,H) ≅ 16 Hz, $Ph_2P\mathit{CH_2}PPh_2$), 3.60 (br d, J(H,H) ≅ 16 Hz, $Ph_2P\mathit{CH_2}PPh_2$), 3.16 (br s, $Ph_2P\mathit{CH_2}PPh_2$), 2.89 (br d, J(H,H) ≅ 16 Hz, $Ph_2P\mathit{CH_2}PPh_2$), 2.71 (br d,

J(H,H) ≅ 16 Hz, $Ph_2P\mathit{CH_2}PPh_2$). $^{31}P\{^1H\}$-NMR (202.5 MHz, CD_2Cl_2, 25 °C): δ 25.4{ddd(or 2 dd), J(P,Rh) = 138 Hz, J(P,Rh) = 141 Hz, J(P,P) = 30 Hz), 13.0 (br d, J(P,Rh) = 132 Hz), −32.2 (dd, J(P,Rh) = 115 Hz), −34.7 (v br). Partial separation, see text, allowed two sets of signals to be identified. Four major signals at: δ 25.8 (dd, J(P,Rh) = 140 Hz, J(P,P) = 30 Hz) and 25.1 (dd, J(P,Rh) = 146 Hz, J(P,P) = 30 Hz); 13.0 (br d, J(P,Rh) = 132 Hz); −32.1 (br, d); −32.4 (br, d), −34.7 (v br) were assigned to **VI** and a second set of three signals at: δ 44.3 (dd, J(P,Rh) = 168 Hz, J(P,P) = 89 Hz); 15.3 (br d, J(P,Rh) = 133 Hz); −0.6 (v br) were assigned to **V**. $^1H\{^{11}B\}$-NMR (500 MHz, CD_3Cl, 25 °C): δ 4.45 (1H, BH), 3.69 (1H, BH), 3.50 (1H, BH), 3.15 (1H, BH), 2.84 (1H, BH), 2.17 (1H, BH), 1.93 (2H, BH).

Table 1
Crystal data and structure refinement for [1-PPh_3-{1,3-(μ-dppm)}-*closo*-1,2-$RhSB_9H_8$] **(IV)**·EtOH and [1,1-(η^2-dppe)-3-(η^1-dppm)-*closo*-1,2-$RhSB_9H_8$] **(VII)**

Compound number	IV	VII
Empirical formula	$C_{45}H_{51}B_9OP_3RhS$	$C_{51}H_{54}B_9P_4RhS$
Formula weight	933.03	1023.08
Temperature (K)	218(2)	223(2)
Wavelength (Å)	0.71073	0.71073
Crystal system	Triclinic	Triclinic
Space group	$P\bar{1}$	$P\bar{1}$
a (Å)	11.8312(2)	10.4180(10)
b (Å)	12.3952(2)	14.7171(14)
c (Å)	17.4196(3)	16.3942(16)
α (°)	71.996(1)	82.010(7)
β (°)	84.696(1)	83.480(7)
γ (°)	73.660(1)	87.340(7)
V (Å^{-3})	2331.33(7)	2471.9(4)
Z	2	2
D_{calc} (Mg m^{-3})	1.329	1.375
Absorption coefficient (mm^{-1})	0.548	0.554
Crystal size (mm)	0.34 × 0.28 × 0.26	0.28 × 0.18 × 0.10
F(000)	960	1052
θ Range for data collection (°)	1.79–30.00	1.97–26.58
Index ranges	$-16 \le h \le 16$, $-16 \le k \le 17$, $-24 \le l \le 24$	$-12 \le h \le 13$, $-18 \le k \le 18$, $-20 \le l \le 20$
Reflections collected	47 315	43 199
Independent reflections	13 088 [R_{int} = 0.021]	10 171 [R_{int} = 0.049]
Max/min transmission	0.8705 and 0.8355	0.9467 and 0.8604
Data/restraints/parameters	13 088/46/592	10 171/0/627
Goodness-of-fit on F^2	1.075	1.187
Final R indices [$I > 2\sigma(I)$] R_1	0.0368	0.0527
WR_2 (all data)	0.1025	0.0868
Largest difference peak and hole (e Å^{-3})	1.038 and −0.427	0.526 and −0.498

Table 2
Selected bond distances (Å) and angles (°) in [1-PPh_3-{1,3-(μ-dppm)}-*closo*-1,2-$RhSB_9H_8$] **(IV)** and [3-(η^1-dppm)-1,1-(η^2-dppe)-*closo*-1,2-$RhSB_9H_8$] **(VII)**

	IV	VII
Bond distances (Å)		
Rh(1)–B(3)	2.078(2)	2.107(3)
Rh(1)–P(2)	2.276(1)	2.265(1)
Rh(1)–P(1)	2.326(1)	2.260(1)
Rh(1)–S(2)	2.357(1)	2.365(1)
Rh(1)–B(6)	2.380(2)	2.379(4)
Rh(1)–B(4)	2.380(2)	2.428(4)
Rh(1)–B(7)	2.442(2)	2.364(4)
S(2)–B(5)	1.874(3)	1.939(4)
S(2)–B(4)	2.001(3)	1.939(4)
B(3)–B(7)	1.699(3)	1.716(5)
B(3)–B(6)	1.736(4)	1.717(5)
B(4)–B(7)	1.846(3)	1.836(5)
B(5)–B(6)	1.850(4)	1.841(5)
B(3)–P(3)	1.887(2)	1.912(4)
Bond angles		
B(3)–Rh(1)–P(2)	87.72(6)	113.88(10)
B(3)–Rh(1)–P(1)	132.91(7)	115.00(10)
P(2)–Rh(1)–P(1)	98.598(19)	84.00(3)
B(3)–Rh(1)–S(2)	117.30(7)	120.97(10)
P(2)–Rh(1)–S(2)	129.36(2)	110.88(3)
P(1)–Rh(1)–S(2)	94.27(2)	105.95(3)
P(3)–B(3)–Rh(1)	118.54(12)	136.61(18)
CH_2–P(3)–B(3)	102.82(11)	113.84(15)
B(9)–B(3)–P(3)	123.58(16)	112.8(2)
B(9)–B(3)–Rh(1)	114.79(12)	110.3(2)
P(3)–CH_2–P(2)/P(4)	110.59(11)	113.80(17)
C(31)–P(2)–Rh(1)	111.12(7)	–
Rh(1)–P(2)–C(2)	–	107.49(10)
Rh(1)–P(1)–C(1)	–	110.39(10)
P(1)–C(1)–C(2)	–	110.1(2)

2.5. *X-ray diffraction [12]*

Data sets were collected using a Bruker SMART CCD area-detector diffractometer at −50 °C. The structures were solved using direct methods and refined by full matrix least squares refinement to convergence in $P\bar{1}$ for both **IV** and **VII**. The cage hydrogen atoms were located and refined freely. All other hydrogen atoms were treated using an appropriate riding model. Structural data are given in Tables 1 and 2.

3. Results and discussion

Treatment of [8,8-$(PPh_3)_2$-*nido*-8,7-$RhSB_9H_{10}$] **(I)** with a three-fold excess of dppm followed by chromatographic workup allows the isolation of the yellow species [8,8-(η^2-dppm)-8-(η^1-dppm)-*nido*-8,7-$RhSB_9H_{10}$] **(II)** in ca. 50% yields. A minor impurity, always obtained in this reaction, is a red species (described later as **V** and **VI**) that eluded characterization [13]. It was not until we

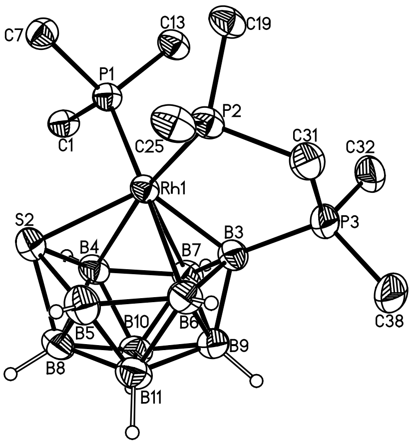

Fig. 1. A view of the molecular structure of **IV** with 50% thermal ellipsoids. Only the *ipso*-carbon atoms on the phenyl groups and the cage H atoms are included to aid clarity. Also missing is a molecule of ethanol.

performed some ligand exchange experiments that clues to the identity of the red compound became clearer to us.

Stirring equimolar mixtures of [8,8-$(PPh_3)_2$-*nido*-8,7-$RhSB_9H_{10}$] (**I**) and [8,8-(η^2-dppm)-8-(η^1-dppm)-*nido*-8,7-$RhSB_9H_{10}$] (**II**) for 3 days in CH_2Cl_2 allowed the isolation of a red species, identified as [1-(PPh_3)\{1,3-(μ-dppm)\}-*closo*-1,2-$RhSB_9H_8$] (**IV**). NMR spectra, and elemental analysis are consistent with the formulation and high-resolution mass spectrometry confirms it with a divergence from the calculated value of 2.2 ppm. Crystals suitable for an X-ray diffraction study were grown from ethanol–CH_2Cl_2 and the structure is given in Fig. 1. It consists of a *closo*-1,2-$RhSB_9$ 11-vertex cluster with a PPh_3 ligand on Rh and a dppm ligand bridging the Rh atom and the closest B atom at position 3. Presumably, during the ligand exchange process between the *nido*-species **I** and **II**, loss of H_2 also occurs resulting in the formation of *closo*-species **IV**. The ^{31}P-NMR spectrum exhibits the expected three signals. These are a doublet of doublets of doublets at 45.8 ppm assigned to the P atom from dppm on Rh, a doublet of doublets at 47.2 ppm assigned to the PPh_3 group on Rh and a single broad resonance assigned to the P atom of the dppm ligand bounded to a cage boron atom. The ^{11}B spectrum exhibits the 1:1:1:2:2:2 pattern expected for the symmetrical *closo*-$RhSB_9$ cage and the $^1H\{^{11}B\}$ spectrum exhibits three resonances assigned to B*H* nuclei in 2:2:4 ratio reflecting some overlap.

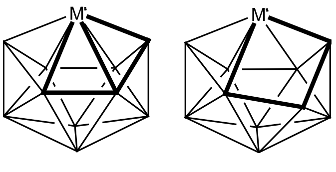

Scheme 2.

A close examination of the structure of **IV** reveals that it is not a simple 11-vertex *closo*-structure. There is no Rh(1)–B(5) bond in the species. This renders an open four-sided 'face' to the molecule reminiscent of the series of *iso*-*nido* 11-vertex clusters which have been discovered in recent years [14]. The difference between our observed structure of **IV** and that for an idealized 11-vertex cluster is illustrated in Scheme 2. The cage is quite distorted in the vicinity of the open face S(2)–Rh(1)–B(6)–B(5). The non-bonded distance Rh(1)–B(5) is 2.678(3) Å, whereas if it were bonding it would be of the order 2.4–2.5 Å, as observed for compound **VII** described below. The stretching of the Rh(1)–B(5) axis is reflected in the shortening of the S(2)–B(6) distance to 3.178(3) Å, whereas in **VII**, a normal octadecahedron, the distance is longer at 3.366(4) Å. The confirmation of **IV** as an *iso*-*nido*-species with an open square face, adds to the number of examples of what may be considered structurally to be 'frozen' intermediates or transition states proposed [15] for the known fluxional process which renders all the vertices in the closed 11-vertex borane $[B_{11}H_{11}]^{2-}$ equivalent on the NMR time-scale [16]. The process is thought to involve diamond-square-diamond rearrangements and the square-faced species is the transition state for such processes. Since the NMR spectra of **IV** do not provide evidence for the structural distortion in that they indicate a plane of symmetry in the $RhSB_9$ cage, the species must be fluxional in solution. In previously described *closo*-species, such as [1,1-(η^2-dppe)-3-(η^1-dppe)-*closo*-1,2-$RhSB_9H_8$] [8] the plane including the two P atoms of the bidentate ligand on Rh, and the Rh atom, is essentially perpendicular to the plane described by the atoms S(2)–Rh(1)–B(3). In the *closo*-species **IV**, however, the system is constrained by the bridging dppm ligand and thus the angle between the planes B(3)–Rh(1)–S(2) and P(2)–Rh(1)–P(1) is 60.3°, suggesting substantial strain in the molecule. Also the angle between the planes P(3)–B(3)–Rh(1) and C(31)–P(3)–B(3) is 146.7°, whereas if the dppm ligand were free at the distal end, the angle would be expected to be close to 180°. Another measure of the extent of strain in the system is the angle Rh(1)–B(3)–P(3) which is 118° whereas in related systems, for example **III** [1b] and **VII** described below, such angles range from 129 to 136°. Clearly **IV** is a strained system and whether this has anything to do with the distortion of the cage is not clear, but it certainly is true that **IV** is the first example of an *iso*-*nido* 11-vertex metallathiaborane.

We were somewhat surprised to observe the dppm ligand bridging between the Rh atom and the boron atom at position 3 in **IV**. We had thought that such bridging might be an intermediate in the hypothetical transfer of a second dppe or dppp ligand from heretofore unobserved dppe or dppp analogues of **II** to form the species **X** shown in Scheme 1. However, we rejected the possibility of such an intermediate for the dppm system in view of the ligand size and also the fact that we observed no analogues of **X** in the case of dppm. We surmised in a previous report that dppm analogues of such species were not observed, because of the shorter dppm ligand disfavoring such a transfer from the Rh in the precursor **II** to the 9-position on the cage [1b]. Reaction of **IV** with dppm in CH_2Cl_2 at r.t. afforded the red compound, which was observed as a minor impurity in the reaction of [8,8-$(PPh_3)_2$-*nido*-8,7-$RhSB_9H_{10}$] (**I**) with dppm, suggesting that perhaps latter species is an analogue of **IV** with a dangling dppm moiety on Rh. Transformation of **II** at r.t. over a period of 7 days also afforded this red compound. Elemental analysis and mass spectrometric data conform to a species with the formula $(dppm)_2RhSB_9H_8$. NMR spectroscopy suggested a mixture but high-resolution mass spectrometry and elemental analysis indicated a composition corresponding to $C_{50}H_{52}B_9P_4RhS$; a $RhSB_9H_8$ cage with two additional dppm ligands attached. The electron count conforms to a *closo*-cluster, assuming that one of the PPh_2 groups is not coordinated to the cage. That would be 12 skeletal electron pairs for an 11-vertex cluster [4]. Our experience suggested that we may have a mixture of [1,1-(η^2-dppm)-3-(η^1-dppm)-*closo*-1,2-$RhSB_9H_8$] (**V**) which is analogous to **XI** and [1,1-(η^2-dppm)-1,3-(μ-dppm)-*closo*-1,2-$RhSB_9H_8$] (**VI**) which is analogous to **IV**.

One can propose a reaction scheme leading to species for which analytical data conforms to that expected for the red compound **V**–**VI**, as shown in Scheme 3. This would involve the transfer of the dangling PPh_2 group on dppm to the cage to form **T**, a transition state containing a very crowded 20 valence electron Rh atom in an electron-rich cluster. Subsequent detachment of a PPh_2 group from Rh can go either to **V′** or **VI′**. This can be followed by loss of H_2 to afford species [1-(η^1-dppm)-1,3-(μ-dppm)-*closo*-1,2-$RhSB_9H_8$] **VI** from **VI′** or [1,1-(η^2-dppm)-3-(η^1-dppm)-*closo*-1,2-$RhSB_9H_8$] **V** from **V′.** If species **V** and **VI** are not interchanging in a solution equilibrium process, then different intermediates are required and this possibility is where we identify the two potential precursors to **V** and **VI** in Scheme 3, as **V′** and **VI′**. Many attempts to solve the structure from diffraction patterns of the nice red crystals which were easy to grow were unsuccessful. One attempt at purification allowed isolation of one of the components in ca. 90% purity which allowed tentative assignments of the resonances in the ^{31}P-NMR spectrum to each isomer.

An examination of the structures of **V** and **VI** given in Scheme 3, indicates that there should be seven resonances in the ^{31}P-NMR spectrum. **V** should have three resonances in 2:1:1 ratio and **VI** should have four resonances in 1:1:1:1 ratio. We observe seven reso-

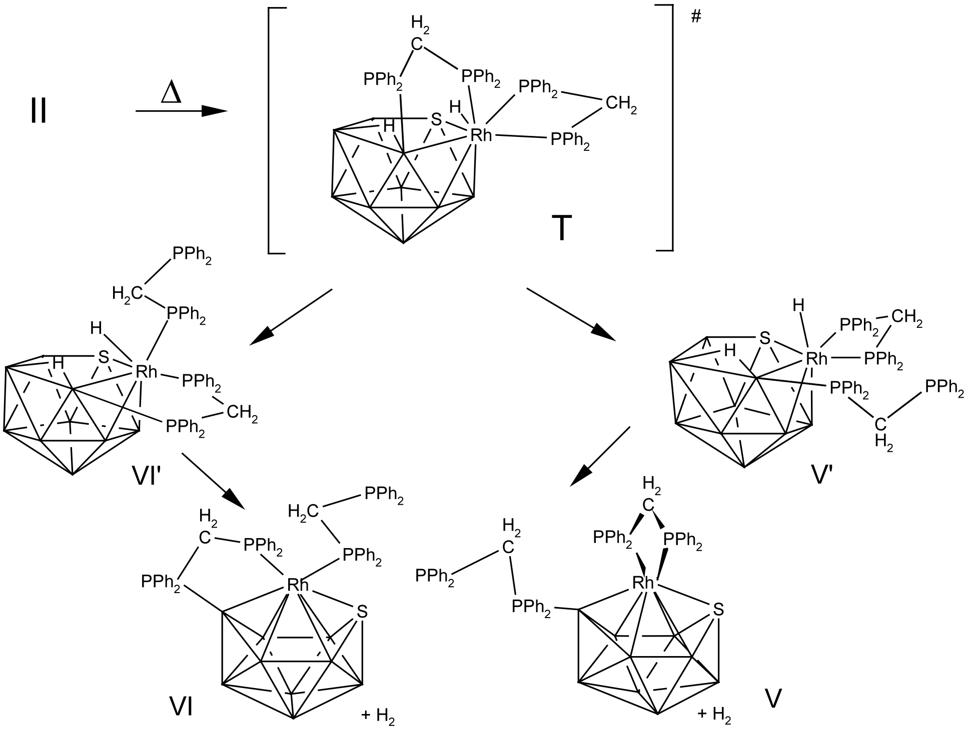

Scheme 3.

nances, and on the basis of the isolation of **VI** in $>90\%$ purity, we are able to assign the spectra and tentative assignments are given in the Section 2. The ^{11}B-NMR spectrum of the mixture consists of nine resonances and the relative areas are consistent with the presence of 18 boron atoms. The gross cage structures for **V** and **VI** are expected to give very similar ^{11}B-NMR spectra but given what we observed for **IV**, it is not unreasonable to expect that **VI** would also be distorted to the *iso-nido* structure thus rendering asymmetry to this molecule, leading to more than six signals. Clearly we do not have the definitive answer to the identity of our 'red' compound but our tentative conclusions are consistent with our observations.

Possible interchange between **V** and **VI** is confirmed by the next experiment we performed. Adding a 50% excess of dppe to a solution of **IV** in CH_2Cl_2, and stirring for 1 h, allows the formation of the ligand exchange product [1,1-(η^2-dppe)-3-(η^1-dppm)-*closo*-1,2-$RhSB_9H_8$] (**VII**). **VII** is formed in 87% yield and identified by elemental analysis, NMR spectroscopy and mass spectrometry. What is interesting about this system is that the dppe ligand, which has replaced the PPh_3 ligand is now bidentate at position-1 and the dppm ligand is dangling. Thus the dppm and the dppe ligands have effectively changed places as indicated in Scheme 4.

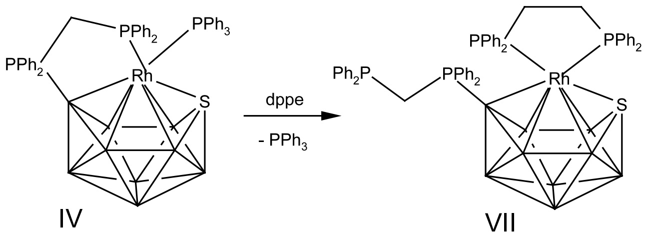

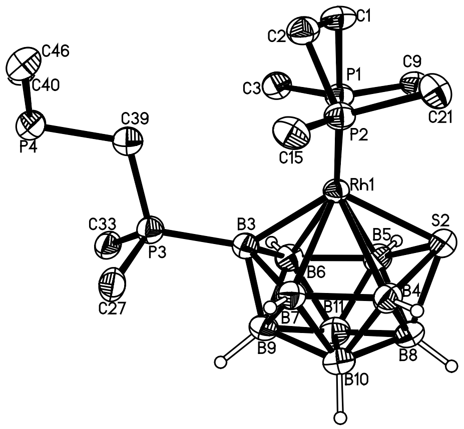

Fig. 2. A view of the molecular structure of **VII** with 50% thermal ellipsoids. Only the cage H atoms are included to aid clarity.

This can arise from a possible mutual rearrangement of pairs of species analogous to **V** and **VI**.

An alternative possibility is that there is no such intermolecular exchange between species types **V** and **VI** but that in the case of addition of dppe to **IV**, initially the PPh_3 is replaced by the dppe ligand which would be expected to become bidentate from considerations of the chelate effect, and the greater stability of bidentate dppe versus dppm. Also the PPh_2 group on a dppe ligand is more nucleophilic than one on a dppm ligand thus the species **VII** is the expected thermodynamic product of this reaction. In other words a dangling PPh_2 group on dppm is more favorable than one on dppe. Crystals of **VII** grown from CH_2Cl_2–pentane were amenable to a single crystal X-ray diffraction study. The structure, given in Fig. 2, confirms the conclusions drawn from the other analytical data. Species **VII** is a conventional 11-vertex *closo*-cluster with the dppe ligand essentially orthogonal to the B(3)–Rh(1)–S(2) plane; the angle between the two planes B(3)–Rh(1)–S(2) and Rh(1)–P(1)–P(2) being 92.6°. Also the orientation of the dangling dppm ligand on position 3 is as expected for a species replacing an *exo*-hydrogen atom; the B(3)–P(3) axis is in the plane of symmetry of the $RhSB_9$ cage. The angle between the planes C(39)–P(3)–B(3) and P(3)–B(3)–Rh(1) is 171.7°, reasonably close to the ideal 180°. Some structural parameters for **IV** and **VII** are given in Table 2, and apart from obvious differences of the two cages and the distortion around the open face of **IV**, they are quite similar.

In summary we have extended the chemistry of the system [8,8-$(PPh_3)_2$-*nido*-8,7-$RhSB_9H_{10}$] (**I**) and in doing so we now understand better the possible modes of rearrangement for bidentate phosphine adducts of the species. We have speculated on possible mechanisms for some of these rearrangements and made some suggestions about likely intermediates. We are extending this chemistry and seek to identify species analogous to **T** in Scheme 2 in order to provide evidence for the existence of such species.

4. Supplementary material

Crystallographic data (excluding structure factors) for the structures reported in this paper have been depositied with the Cambridge Crystallographic Cata Center: Compound **IV**, CCDC no. 179102 and Compound **VII**, CCDC no. 179101. Copies of the information may be obtained free of charge from: The Director, CCDC, 12 Union Road, Cambridge CB2 1EZ, UK (Fax: +44-1223-336033; e-mail: deposit@ccdc.cam.ac.uk or www: http://www.ccdc.cam.ac.uk).

Acknowledgements

We acknowledge the NSF (grant Nos. CHE-9727570), the Missouri Research Board and UM-St. Louis for research grants to L.B., and the NSF and the UM-St. Louis Center for Molecular Electronics and the Missouri Research Board for funds which help purchase the NMR, XRD and MS facilities.

References

[1] (a) Previous papers in the series are: R. Macías, N.P. Rath, L. Barton, Angew. Chem. Int. Ed. Engl. 38 (1999) 162;
(b) R. Macías, N.P. Rath, L. Barton, Organometallics 18 (1999) 3637;
(c) O. Volkov, N.P. Rath, L. Barton, Inorg. Chem. Commun. 5 (2002) 127.

[2] C.W. Jung, M.F. Hawthorne, J. Am. Chem. Soc. 102 (1980) 3024.

[3] (a) G. Ferguson, M.C. Jennings, A.J. Lough, S. Coughlan, T.R. Spalding, J.D. Kennedy, X.L.R. Fontaine, B. Štíbr, J. Chem. Soc. Chem. Commun. (1990) 891;
(b) S. Coughlan, T.R. Spalding, G. Ferguson, J.F. Gallagher, A.J. Lough, X.L.R. Fontaine, J.D. Kennedy, B. Štíbr, J. Chem. Soc. Dalton Trans. (1992) 2865.

[4] (a) R.E. Williams, Adv. Inorg. Chem. Radiochem. 18 (1976) 67;
(b) K. Wade, Adv. Inorg. Chem. Radiochem. 18 (1976) 60;
(c) R.W. Rudolph, Acc. Chem. Res. 9 (1976) 446.

[5] K.J. Adams, T.D. McGrath, G.M. Rosair, A.S. Weller, A.J. Welch, J. Organomet. Chem. 550 (1998) 315.

[6] G. Ferguson, A.J. Lough, S. Coughlan, T.R. Spalding, Acta Crystallogr. Sect. C: Cryst. Struct. Commun. Sect. C 48 (1992) 440.

[7] M. Murphy, T.R. Spalding, G. Ferguson, J.F. Gallagher, Acta Crystallogr. Sect. C: Cryst. Struct. Commun. Sect. C 48 (1992) 638.

[8] K.J. Adams, T.D. McGrath, R.L. Thomas, A.S. Weller, A.J. Welch, J. Organomet. Chem. 527 (1997) 283.

[9] D.F. Shriver, M.A. Drezdon, The Manipulation of Air-Sensitive Compounds, Wiley, New York, 1986.

[10] R.W. Rudolph, W.R. Pretzer, Inorg. Synth. 22 (1983) 226.

[11] J.A. Osborn, G. Wilkinson, Inorg. Synth. 28 (1990) 77.

[12] (a) SHELXTL Software Package, 2001. Bruker Analytical X-ray Division, Madison, WI.
(b) For further details see experimental section in: P. McQuade, K. Hupp, J. Bould, H. Fang, N.P. Rath, R. Ll. Thomas, L. Barton, Inorg. Chem. 38 (1999) 5415.

[13] R. Macías, L. Barton, unpublished observations.

[14] (a) M. Bown, X.L.R. Fontaine, N.N. Greenwood, J.D. Kennedy, M. Thornton-Pett, Organometallics 6 (1987) 2254;
(b) K. Nestor, X.L.R. Fontaine, N.N. Greenwood, J.D. Kennedy, J. Plesek, B. Štíbr, M. Thornton-Pett, Inorg. Chem. 28 (1989) 2219;
(c) J. Bould, N.P. Rath, L. Barton, Acta. Crystallogr. Sect. C 53 (1997) 416;
(d) M. Bown, B. Gruner, B. Štíbr, X.L.R. Fontaine, M. Thornton-Pett, J.D. Kennedy, J. Organomet. Chem. 614/615 (2000) 269.

[15] D.A. Kleier, D.A. Dixon, W.N. Lipscomb, Inorg. Chem. 17 (1978) 166.

[16] (a) E.I. Tolpin, W.N. Lipscomb, J. Am. Chem. Soc. 95 (1973) 2384;
(b) R.E. Weirsema, M.F. Hawthorne, Inorg. Chem. 12 (1973) 785.